Vapor-Liquid Equilibrium of Binary Systems Containing Cyano-based Ionic Liquids and CO₂: SAFT-γ GC EoS Modeling

Ashrafmansouri, Seyedeh Saba*⁺

Department of Chemical Engineering, University of Larestan, Lar, I.R. IRAN

ABSTRACT: *The unusual thermodynamic behavior of ionic liquid (IL)+CO₂ mixtures has challenged their theoretical modeling. In this paper, a SAFT-γ equation-based group contribution method (SAFT-γ GC EoS) is used to predict the vapor-liquid equilibrium (VLE) of these mixtures. The binary systems containing CO₂ and 1-butyl-3-methyl-imidazolium-thiocyanate ([bmim][SCN]), 1-ethyl-3-methylimidazolium dicyanamide ([emim][DCA]), 1-butyl-3-methylimidazolium dicyanamide ([bmim][DCA]), 1-hexyl-3-methylimidazolium dicyanamide ([hmim][DCA]), 1-ethyl-3-methylimidazolium tricyanomethanide ([emim][TCM]), 1-butyl-3-methylimidazolium tricyanomethanide ([bmim][TCM]) or 1-hexyl-3-methylimidazolium tetracyanoborate ([hmim][TCB]) are divided into the functional groups of CO₂, cyano-based anion, CH₂, CH₃ and imidazolium-based cationic head. Some new SAFT-γ parameters are optimized at temperatures from 283.15 to 373.15 K and at pressures up to about 20 MPa. The observation of an average error of 1.86% between experimental and estimated bubble pressures indicates the desirable performance of SAFT-γ GC EoS to predict the VLE of CO₂+imidazolium-, cyano-based ionic liquid mixtures.*

KEYWORDS: *CO₂; Ionic liquid; Cyano; SAFT; Group Contribution.*

INTRODUCTION

The high solubility of carbon dioxide in Ionic Liquids (ILs), low vapor pressure of ILs and easier CO₂ removal from ILs compared to its separation from conventional industrial solvents make ILs suitable candidates for designing CO₂-capture processes [1-5]. It is clear that experimental and theoretical data on CO₂ solubility in ILs are necessary to develop CO2-capture technologies by these liquids. Since experimental measurements are not practical for all members of ILs' family (about 10^{18} members), turning to theoretical methods for predicting the CO₂ solubility in them can be very useful [6-8]. However, due to the unusual

behavior of dew and bubble pressure curves of ionic liquid+CO₂ mixtures compared to CO₂+conventional liquid systems, predicting the thermodynamic behavior of these binary mixtures is very challenging [9, 10].

Modeling the thermodynamic behavior of IL systems based on classic models such as cubic Equations of State (EoS) requires various temperature- and/or composition-dependent parameters. However, these models can't observe the true nature of IL molecules because of considering the anionic and cationic parts of IL structure together as a neutral pair. The positive and negative ions

have polarity and ability to associate that these two factors are not explicitly considered in the cubic equations of state. Moreover, cubic EoS needs knowledge of critical parameters. The critical properties of most ILs can't be determined experimentally because most of these materials decompose as their temperature approaches normal boiling point. Therefore, their critical parameters are only indirectly predicted with large uncertainties, which leads to a fundamental problem [9, 10].

In addition, most classical equations have been used for a limited number of ILs, and their use for other members of IL family can lead to significant deviations from experimental data [11]. Since the IL family has many common functional groups among its various members, the use of group contribution (GC) method is a useful approach to model the thermodynamic behavior of this family. In this method, by specifying the parameters of a number of functional groups, it will be possible to predict the thermodynamic behavior of even those ILs that have not been studied in model construction. Furthermore, some GC methods do not even require critical properties [9, 10]. Because of these advantages, GC methods in IL research fields have become popular [12-14]

Among various thermodynamic models, equations based upon statistical associating fluid theory (SAFT) have also been very successful in modeling the phase behavior of CO_2+IL mixtures [9, 10, 15-23]. *Llovell et al.* [15, 16] employed soft-SAFT approach to predict gas absorption (CO, CH_4, H_2, CO_2, H_2S or SO_2) in some imidazolium-based ILs with anions of [BF_4], [PF_6], [Tf_2N] or [$MeSO_4$]. *Ferreira et al.* [17] also applied the soft-SAFT EoS to describe the VLE of some systems including fluorinated ILs+atmospheric gases. *Alkhatib et al.* [18] also investigated capacity of CO_2 capturing by some ILs with the soft-SAFT equation. *Ghotbi et al.* [19] estimated solubility of acid gases (CO_2 and H_2S) in [C_8mim][PF_6] and [C_8mim][Tf_2N] by means of PC-SAFT EoS at low pressures. Al-fnaish and Lue [20] also predicted solubility of CO_2 and H_2S in some methylimidazolium bis (trifluoromethylsulfonyl) imide ILs ([$C_n$mim][Tf_2N] where n = 2, 4, 6, and 8) using PC-SAFT equation. They found that considering a 4-site association scheme with two donors and two acceptors in the structure of IL provided the best results for almost all the investigated acid gases-IL binary systems, with an average absolute relative deviation (AARD) of 2.76%–6.62% for H_2S-ILs systems

and 1.54%–4.98% for CO_2-IL systems [20]. In addition, *Ayad et al.* [21] modeled the VLE of CO_2 in three tricyanomethanide based ILs with different cations ([BMIM][TCM], [BMPY][TCM] or [BMPYR][TCM]) based upon PC-SAFT EoS and observed higher CO_2 solubility in pyridinium-based ILs [21]. *Alcantara et al.* [22] used sPC-PSAFT EoS to predict carbon dioxide solubility in three ILs with ethanolamine cations and butanoate anions. Their model was able to estimate the CO_2 solubility at high pressures with good accuracy, but low-pressure predictions were under experimental data [22]. *Alcantara et al.* [22] also found that increase in carbon chain length, bonded to amine group, promotes higher CO_2 solubility at medium-high pressures but lower CO_2 solubility at low pressures [22]. *Loreno et al.* [23] successfully predicted solubility of carbon dioxide or methane in some imidazolium-based ILs ([$C_n$mim][BF_4], [$C_n$mim][PF_6] and [$C_n$mim][Tf_2N]) with GC-sPC-SAFT equation within a vast pressure range. They found that considering speed of sound data and association parameters are the key factors in optimization process [23].

Considering ability of SAFT models and comprehensiveness of GC approaches, we studied the thermodynamic behavior of some pure imidazolium-based ILs and their binary mixtures with CO_2 by a combination of SAFT-γ EoS and a GC technique [8-10]. The SAFT-γ GC method doesn't need the critical properties of ILs and by breaking down the IL molecule into the chemical groups of cationic head, cationic alkyl groups of CH_2 and CH_3, and anionic groups, can be predictive for the thermodynamic behavior of a larger number of ILs [9]. Moreover, the model more realistically shows the geometric configuration of molecules by defining the shape factor parameter. This parameter specifies the contribution of a specific segment among the whole molecular structure and allows the fused segments to form heteronuclear molecules [9, 10, 24]. The SAFT-γ model can consider various interactions in the systems of carbon dioxide and ILs (particularly the associations between cationic head and anionic group, associations between CO_2 and anionic group and self-association between CO_2 molecules) [9].

In our previous researches [9, 10], the density and CO_2 solubility of some imidazolium-based ILs with anions of [BF_4], [PF_6], [Tf_2N], [$MeSO_3$], [$MeSO_4$], [$EtSO_4$] or [CF_3SO_3] were studied by SAFT-γ equation. Moreover, in our recent work [8], density and second-order derivative

properties of some imidazolium-, cyano-based ILs were estimated with the SAFT-γ model. In the present paper, to extend the data bank of SAFT-γ parameters, some new parameters of SAFT-γ GC EoS for seven systems of CO_2+imidazolium-based ILs with cyano-based anions of [SCN], [DCA], [TCM] or [TCB] are optimized.

THEORETICAL SECTION

In the SAFT-γ GC EoS, each functional group (k or l) is made of v_k^* fused segments which are specified by parameters of segment diameter (σ_{kk}), shape factor (S_k), dispersion energy and range (ε_{kk} and λ_{kk}). The combination of different functional groups makes the components i or j. To define interactions between groups l and k, the association energy parameters (ε_{klab}^{HB} and r_{klab}^c, $a = 1,\ldots,NST_k$; $b = 1,\ldots,NST_l$) and the dissimilar potential parameters ($\sigma_{kl}.\varepsilon_{kl}.\lambda_{kl}$) are taken into consideration [9, 10, 24, 25].

In this paper, the binary mixture of CO_2 and IL is divided into the single-segment functional groups of CO_2, anion, cationic head, CH_2 and CH_3. One electropositive site on the cationic head group, two electronegative sites on the anionic group, one electropositive and two electronegative sites on the CO_2 molecule are taken into consideration to describe the anion-CO_2, CO_2-CO_2 and anion-cationic head association interactions [9, 10].

Considering the ideal Helmholtz energy (A^{ideal}), Helmholtz energy of hard-sphere repulsions and dispersions (A^{mono}), Helmholtz energy of connections of heteronuclear segments to each other (A^{chain}) and Helmholtz energy of association bonding (A^{assoc}) between electronegative (type a) and electropositive sites (type b), the SAFT-γ GC equation is defined by Eq. (1) [24].

$$\frac{A}{Nk_BT} = \frac{A^{ideal}}{Nk_BT} + \frac{A^{mono}}{Nk_BT} + \frac{A^{chain}}{Nk_BT} + \frac{A^{assoc}}{Nk_BT} \tag{1}$$

Where k_B, T and N are respectively Boltzmann constant, temperature and molecules' number. In the following, the association Helmholtz energy is introduced in Eq. (2). The terms of A^{ideal}, A^{mono} and A^{chain} are provided in Refs. [9, 24].

$$\frac{A^{assoc}}{Nk_BT} = \sum_{i=1}^{NC} x_i \sum_{k=1}^{NG} v_{k,i} \sum_{a=1}^{NST_k} n_{ka}\left(\ln X_{ika} + \frac{1-X_{ika}}{2}\right) \tag{2}$$

Where NC, NG and NST_k are respectively components' number, groups' number and association site types' number of group k. Furthermore, x_i, $v_{k,i}$, n_{ka} and X_{ika} are

respectively mole fraction of component i, number of group k (in component i), number of electronegative sites (on group k) and the not-associated share of component i (at electronegative site of group k). X_{ika} is determined by the following equation [9, 10, 24]:

$$X_{ika} = \frac{1}{1 + \sum_{j=1}^{NC}\sum_{l=1}^{NG}\sum_{b=1}^{NST_l} \rho x_j v_{l,j} n_{lb} X_{jlb} \Delta_{ijklab}} \tag{3}$$

Where ρ and Δ_{ijklab} are respectively the number density and the function of association strength. The Δ_{ijklab} is available in our previous publications [9, 10]. Pressure (P), chemical potential of component i (μ_i) and fugacity coefficient of component i ($\hat{\varphi}_i$) are calculated based on usual thermodynamics equations [9, 24]:

$$P = \frac{\sum_{i=1}^{NC} N_i \mu_i - A}{V} \tag{4}$$

$$\mu_i = -\left(\frac{\partial A}{\partial N_i}\right)_{N_{j \neq i}, V, T} \tag{5}$$

$$\ln \widehat{\varphi}_i = \frac{\mu_i^{res}}{Nk_BT} - \ln Z \tag{6}$$

In Eqs. (4)-(6), V, N_i and Z are respectively volume of system, number of molecules of component i and compressibility factor. μ_i^{res} is residual chemical potential of component i which is calculated by [24]:

$$\frac{\mu_i^{res}}{k_BT} = \frac{\mu_i^{mono}}{k_BT} + \frac{\mu_i^{chain}}{k_BT} + \frac{\mu_i^{assoc}}{k_BT} \tag{7}$$

where μ_i^{mono}, μ_i^{chain} and μ_i^{assoc} are respectively chemical potential of component i related to hard-sphere repulsions and dispersions, chemical potential of component i due to connections of heteronuclear segments to each other and chemical potential of component i related to association bonding. In the following, μ_i^{assoc} is introduced in Eq. (8). μ_i^{mono} and μ_i^{chain} are available in Ref. [24].

$$\frac{\mu_i^{assoc}}{k_BT} = \sum_{k=1}^{NG}\sum_{a=1}^{NST_k} v_{k,i} n_{ka}\left(\ln X_{ika} + \frac{1 - X_{ika}}{2}\right)$$
$$+ \sum_{j=1}^{NC}\sum_{k=1}^{NG}\sum_{a=1}^{NST_k} x_j N v_{k,j} n_{ka}\left(\frac{1}{X_{jka}} - \frac{1}{2}\right)\frac{\partial X_{jka}}{\partial N_i} \tag{8}$$

In this research, the association energy parameters (ε_{klab}^{HB}, r_{klab}^c) and binary interaction parameters (k_{ij}) between CO_2 and anions of [SCN, [DCA], [TCM] or [TCB] are optimized

based on Eq. (9) and Differential Evolution (DE) optimization method in MATLAB environment [9, 10, 26].

$$\text{Obj. Func} = \frac{1}{ND} \times \sqrt{\sum_{i=1}^{ND} \left(\frac{P_i^{Exp.} - P_i^{Calc.}}{P_i^{Exp.}} \right)^2} \qquad (9)$$

In Eq. (9), $P_i^{Calc.}$ and $P_i^{Exp.}$ are, respectively, the calculated and the experimental bubble pressures and *ND* is the number of data [9, 10].

The group parameters of anions, cationic head, CO_2 and the parameters of cationic head-anion and CO_2-CO_2 association bondings, the binary interaction parameters among CO_2 and cationic head, CH_3 or CH_2 have been optimized in our previous publications [9, 10]. The group parameters of CH_2 and CH_3 are also accessible in Ref. [25]. The dissimilar potential parameters (σ_{kl}. ε_{kl}. λ_{kl}) are also calculated based upon arithmetic relations [9, 10, 24].

RESULTS AND DISCUSSION

The optimized parameters of association energy (ε_{klab}^{HB}) and its distance (r_{klab}^c) are available in Table 1. These parameters are related to the association bonding among the anionic groups and CO_2. In the present paper, the parameter of binary interaction (k_{ij}) among the anionic group and CO_2 is considered as a linear function of temperature (Eq. (10)). The constants of this linear function are provided in Table 2.

$$k_{ij} = c_1 + c_2 T \qquad (10)$$

Table 3 presents the average absolute relative deviation (*AARD*%) values between experimental and estimated bubble pressures for studied ILs. The optimization process was done for chemical systems of [bmim][SCN]+ CO_2, [bmim][DCA]+ CO_2, [bmim][TCM]+ CO_2 or [hmim][TCB]+ CO_2, respectively based on experimental data of *Kim et al.* [27], *Carvalho et al.* [28], *Zubeir et al.* [29] and *Mota-Martinez et al.* [30]. *AARD*% is determined by:

$$\text{AARD}\% = \frac{1}{ND} \times \sum_{i=1}^{ND} \left| \frac{P_i^{Exp.} - P_i^{Calc.}}{P_i^{Exp.}} \right| \times 100 \qquad (11)$$

After optimizing the SAFT-γ parameters, the model with the optimum parameters was applied to predict VLE of CO_2+ionic liquid systems which their experimental bubble pressures had not been applied in the fitting step. Table 3 indicates all correlation and prediction errors. The average error of 1.86% was obtained for 316 data points.

TABLE 1: The optimized association parameters

Groups	$\varepsilon^{HB}/k_B(K)$	$r^c(A°m)$
[SCN]- CO_2	710.3726	4.6123
[DCA]- CO_2	749.9463	5.6868
[TCM]- CO_2	790.2995	3.5000
[TCB]- CO_2	643.3392	4.3370

TABLE 2: The optimized constants of Eq. (10) to determine k_{ij}

Groups	c_1	c_2
[SCN]- CO_2	-0.1989	0.0013
[DCA]- CO_2	-0.1840	0.0012
[TCM]- CO_2	-0.1648	0.0004
[TCB]- CO_2	-0.0345	0.0005

Moreover, Fig.s 1-4 indicate experimental and SAFT-γ predicted bubble pressures of binary systems of CO_2+[bmim][SCN], [bmim][DCA], [emim][TCM] or [hmim][TCB] at different temperatures and CO_2 mole fractions. Experimental data of *Kim et al.* [1] (for CO_2+[bmim][SCN] or [emim][TCM]), *Carvalho et al.* [28] (for CO_2+[bmim][DCA]) and *Mota-Martinez et al.* [30] (for CO_2+[hmim][TCB]) have been shown in these Fig.s.

Table 3 and Fig.s 1-4 show good potential of SAFT-γ model to estimate the bubble pressure of carbon dioxide+imidazolium-, cyano-based ionic liquid systems. New parameters of SAFT-γ equation optimized in the present reseach can be added to the previous SAFT-γ data bank [8-10] for ionic liquids. Using these group parameters, the phase behavior of ILs (even those their experimental data have not been employed in the optimization step while their constituent functional groups are in common with the groups in the SAFT-γ data bank) can be predicted with acceptable reliability without using any additional parameter. It is worth to mention that in this work, even binary interaction parameters (k_{ij}) have also been described based upon the group contribution concept to preserve the model's comprehensiveness.

CONCLUSIONS

In this paper, the SAFT-γ GC EoS was extended to describe the VLE of binary systems including CO_2 and imidazolium-, cyano-based ILs. The CO_2+IL mixtures were divided into the functional groups of CH_3, CH_2, cationic head, anion and CO_2, and some group parameters of SAFT-γ GC EoS were optimized using the Differential Evolution algorithm. Considering the electronegative and

TABLE 3- AARD% in bubble pressures

IL+CO₂	Temperature (K)	Pressure (MPa)	AARD %	No.⁺	Reference
[bmim][SCN]+CO_2	303.15-373.15	0.70-20.72	1.92*	48	Kim et al. [27]
[emim][DCA]+CO_2	303.15-373.15	0.88-10.79	6.36#	30	Kim et al. [1]
[bmim][DCA]+CO_2	293.41-363.18	1.02-13.10	1.95*	28	Carvalho et al. [28]
[bmim][DCA]+CO_2	298.2-333.3	1.41-11.48	3.19#	18	Aki et al. [31]
[hmim][DCA]+CO_2	303.15-373.15	1.13-11.92	4.27#	27	Cho et al. [32]
[emim][TCM]+CO_2	303.15-373.15	0.59-11.06	0.80#	40	Kim et al. [1]
[bmim][TCM]+CO_2	283.13-363.14	0.52-9.48	0.26*	59	Zubeir et al. [29]
[hmim][TCB]+CO_2	288.48-363.91	0.27-11.24	0.58*	53	Mota-Martinez et al. [30]
[hmim][TCB]+CO_2	313.15	0.54-7.11	0.01#	13	Zakrzewska and Nunes da Ponte [33]

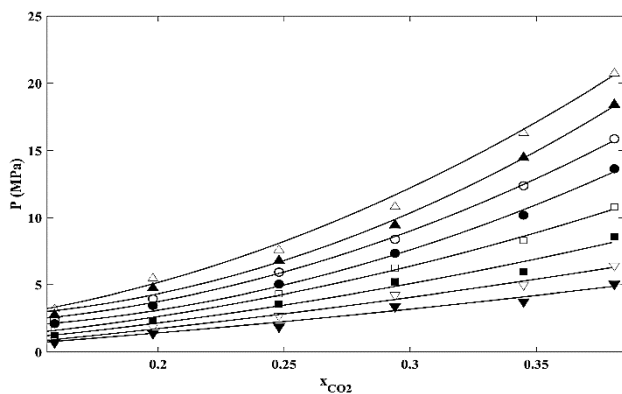** Correlations using SAFT-γ equation, # Predictions using SAFT-γ equation*

Fig. 1: Predicted and experimental bubble pressures of [bmim][SCN] versus CO_2 mole fraction at several temperatures. The solid curves are SAFT-γ estimations and the marks are experimental data of Kim et al. [1] at temperatures of 303.15 (▼), 313.15 (▽), 323.15 (■), 333.15 (□), 343.15 (●), 353.15 (○), 363.15 (▲) and 373.15 (△) K.
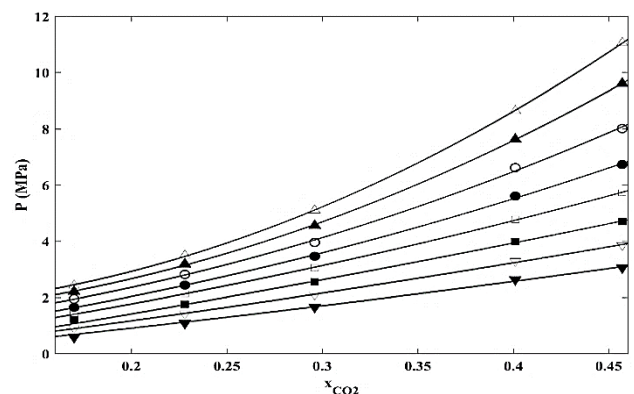

Fig. 3: Predicted and experimental bubble pressures of [emim][TCM] vs. CO_2 mole fraction at several temperatures. The solid curves are SAFT-γ estimations and the marks are experimental data of Kim et al. [1] at temperatures of 303.15 (▼), 313.15 (▽), 323.15 (■), 333.15 (□), 343.15 (●), 353.15 (○), 363.15 (▲) and 373.15 (△) K.
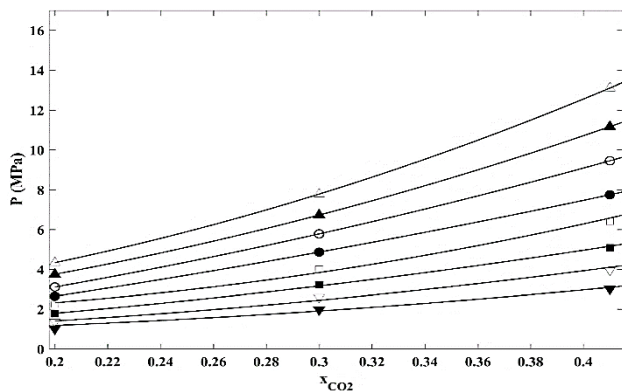

Fig. 2: Predicted and experimental bubble pressures of [bmim][DCA] versus CO_2 mole fraction at various temperatures. The solid curves are SAFT-γ estimations and the signs are experimental data of Carvalho et al. [28] at temperatures of 293.41 (▼), 303.43 (▽), 313.24 (■), 323.15 (□), 333.04 (●), 343.15 (○), 353.10 (▲) and 363.18 (△) K.
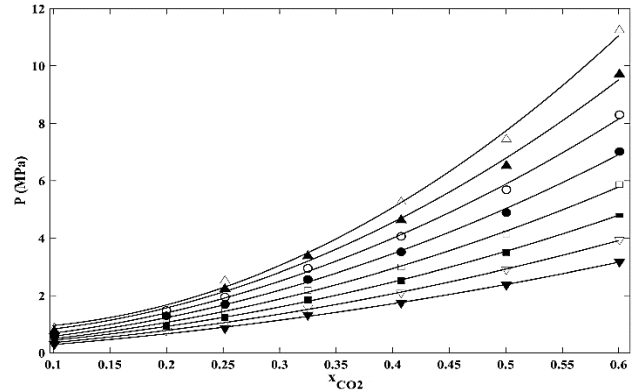

Fig. 4: Predicted and experimental bubble pressures of [hmim][TCB] vs. CO_2 mole fraction at various temperatures. The solid curves are SAFT-γ estimations and the marks are experimental data of Mota-Martinez et al. [30] at temperatures of 293.63 (▼), 303.62 (▽), 313.64 (■), 323.65 (□), 333.66 (●), 343.69 (○), 353.77 (▲) and 363.91 (△) K.

electropositive association sites on the functional groups of anion, cationic head and CO_2, it was possible to take into account the anion-CO_2, CO_2-CO_2 and anionic-cationic head association interactions. Eight association energy parameters and its range, and four binary interaction parameter between CO_2 and cyano anions were optimized in this research. The comparison between experimental and predicted bubble pressures showed the average absolute relative deviation of 1.86% for 316 data points. The results indicated the power of SAFT-γ GC EoS to model the thermodynamic behavior of ionic liquid+CO_2 systems within the temperature and pressure ranges of 283.15-373.15 K and 0.27-20 MPa. The SAFT-γ GC EoS with the optimized parameters showed very good performance to predict the VLE

Acknowledgement

Nomenclature

energy of Helmholtz	A
average absolute relative deviation (in percentage)	AARD%
constant of Eq. (10)	c
Boltzmann constant	k_B
binary interaction between different groups	k_{ij}
number of electronegative or electropositive association sites	n
molecules' number	N
components' number	NC
number of experimental data	ND
group types' number	NG
number of association site types	NST
pressure	P
cut-off distance	r_{klab}^c
shape factor	S
temperature	T
volume	V
number of group k in constituent i	$v_{k,i}$
fused segments' number of group k	v_k^*
mole fraction of a component	x
non-associated portion of a constituent	X
compressibility factor	Z
energy of dispersion	ε
energy of association	$ε^{HB}$
range of dispersion	λ

chemical potential	μ
density	ρ
segment diameter	σ
fugacity coefficient	φ
contribution of association energy	assoc
contribution of molecules' formation from hetero-nuclear segments	chain
Calculated (predicted) property	Calc.
Experimental property	Exp.
contribution of ideal Helmholtz energy	ideal
contribution of hard-sphere dispersions and repulsions	mono
electronegative site	a
electropositive site	b
data, component	i
component	j
type of group	k
type of group	l

References

[1] Kim J.E., Kim H.J., Lim J.S., Solubility of Co_2 in Ionic Liquids Containing Cyanide Anions: [C_2mim][SCN], [C_2mim][N(CN)$_2$], [C_2mim][C(CN)$_3$], *Fluid Phase Equilibria,* **367:** 151-158 (2014).

[2] Kazmi S., Awan Z., Hashmi S., Simulation Study of Ionic Liquid Utilization for Desulfurization of Model Gasoline, *Iranian Journal of Chemistry and Chemical Engineering (IJCCE),* **38(4):** 209-221 (2019).

[3] Pazuki G., Zare Khafri H., Naderifar A., Liquid-Liquid Extraction of Toluene from Heptane Using [Emim][Ntf$_2$] Ionic Liquid: Experimental and Extensive Thermodynamics Study, *Iranian Journal of Chemistry and Chemical Engineering (IJCCE)*, **41(3):** 913-924 (2021).

[4] Philip F.A., Henni A., Enhancement of Post-Combustion CO_2 Capture Capacity by Incorporation of Task-Specific Ionic Liquid into Zif-8, *Microporous and Mesoporous Materials*, **330:** 111580 (2021).

[5] Kazmi B., Haider J., Ammar Taqvi S.A., Qyyum M.A., Ali S.I., Hussain Awan Z.U., Lim H., Naqvi M., Naqvi S.R., Thermodynamic and Economic Assessment of Cyano Functionalized Anion Based Ionic Liquid for Co2 Removal from Natural Gas Integrated with, Single Mixed Refrigerant Liquefaction Process for Clean Energy, *Energy* **239(Part E):** 122425 (2021).

[6] Shen G., Held C., Lu X., Ji X., Modeling Thermodynamic Derivative Properties of Ionic Liquids with Epc-Saft, *Fluid Phase Equilibria,* **405:** 73-82 (2015).

[7] Sun Y., Schemann A., Held C., Lu X., Shen G., Ji X., Modeling Thermodynamic Derivative Properties and Gas Solubility of Ionic Liquids with Epc-Saft, *Industrial & Engineering Chemistry Research,* **58(19):** 8401-8417 (2019).

[8] Ashrafmansouri S.-S., Modeling the Density and the Second-Order Thermodynamic Derivative Properties of Imidazolium-, Cyano-Based Ionic Liquids Using the Saft-Γ Eos, *Fluid Phase Equilibria,* **548:** 113190 (2021).

[9] Ashrafmansouri S.-S., Raeissi S., Modeling Gas Solubility in Ionic Liquids with the Saft-Γ Group Contribution Method, *The Journal of Supercritical Fluids,* **63:** 81-91 (2012).

[10] Ashrafmansouri S.-S., Raeissi S., Extension of Saft-Γ to Model the Phase Behavior of CO_2+Ionic Liquid Systems, *Fluid Phase Equilibria,* **538:** 113026 (2021).

[11] Rostami A., Baghban A., Shirazian S., On the Evaluation of Density of Ionic Liquids: Towards a Comparative Study, *Chemical Engineering Research and Design,* **147:** 648-663 (2019).

[12] Gholizadeh F., Sabzi F., Prediction of CO_2 Sorption in Poly(Ionic Liquid)S Using ANN-GC and ANFIS-GC Models, *International Journal of Greenhouse Gas Control,* **63:** 95-106 (2017).

[13] Kardani M.N., Baghban A., Sasanipour J., Mohammadi A.H., Habibzadeh S., Group Contribution Methods for Estimating CO_2 Absorption Capacities of Imidazolium and Ammonium-Based Polyionic Liquids, *Journal of Cleaner Production,* **203:** 601-618 (2018).

[14] Song Z., Shi H., Zhang X., Zhou T., Prediction of CO_2 Solubility in Ionic Liquids Using Machine Learning Methods, *Chemical Engineering Science,* **223:** 115752 (2020).

[15] Llovell F., Marcos R.M., MacDowell N., Vega L.F., Modeling the Absorption of Weak Electrolytes and Acid Gases with Ionic Liquids Using the Soft-Saft Approach, *The Journal of Physical Chemistry B,* **116(26):** 7709-7718 (2012).

[16] Llovell F., Oliveira M.B., Coutinho J.A.P., Vega L.F., Solubility of Greenhouse and Acid Gases on the [C_4mim][$MeSO_4$] Ionic Liquid for Gas Separation and CO_2 Conversion, *Catalysis Today,* **255:** 87-96 (2015).

[17] Ferreira M.L., Llovell F., Vega L.F., Pereiro A.B., Araújo J.M.M., Systematic Study of the Influence of the Molecular Structure of Fluorinated Ionic Liquids on the Solubilization of Atmospheric Gases Using a Soft-Saft Based Approach, *Journal of Molecular Liquids,* **294:** 111645 (2019).

[18] Alkhatib I.I.I., Ferreira M.L., Alba C.G., Bahamon D., Llovell F., Pereiro A.B., Araújo J.M.M., Abu-Zahra M.R.M., Vega L.F., Screening of Ionic Liquids and Deep Eutectic Solvents for Physical CO2 Absorption by Soft-Saft Using Key Performance Indicators, *Journal of Chemical & Engineering Data,* **65(12):** 5844-5861 (2020).

[19] Ghotbi C., Safavi M., Tavakolmoghadam M., Modeling the Solubility of Acid Gases in Ionic Liquids, *Gas Processing Journal,* **2(2):** 53-66 (2014).

[20] Al-Fnaish H., Lue L., Modelling the Solubility of H_2S and CO_2 in Ionic Liquids Using PC-SAFT Equation of State, *Fluid Phase Equilibria,* **450:** 30-41 (2017).

[21] Ayad A., Negadi A., Mutelet F., Carbon Dioxide Solubilities in Tricyanomethanide-Based Ionic Liquids: Measurements and Pc-Saft Modeling, *Fluid Phase Equilibria,* **469:** 48-55 (2018).

[22] Alcantara M.L., Ferreira P.I.S., Pisoni G.O., Silva A.K., Cardozo-Filho L., Lião L.M., Pires C.A.M., Mattedi S., High Pressure Vapor-Liquid Equilibria for Binary Protic Ionic Liquids+Methane or Carbon Dioxide, *Separation and Purification Technology,* **196:** 32-40 (2018).

[23] Loreno M., Reis R.A., Mattedi S., Paredes M.L.L., Predicting the Solubility of Carbon Dioxide or Methane in Imidazolium-Based Ionic Liquids with Gc-Spc-Saft Equation of State, *Fluid Phase Equilibria,* **479:** 85-98 (2019).

[24] Lymperiadis A., Adjiman C.S., Jackson G., Galindo A., A Generalisation of the Saft-Γ Group Contribution Method for Groups Comprising Multiple Spherical Segments, *Fluid Phase Equilibria,* **274(1):** 85-104 (2008).

[25] Lymperiadis A., Adjiman C.S., Galindo A., Jackson G., A Group Contribution Method for Associating Chain Molecules Based on the Statistical Associating Fluid Theory (Saft-Γ), *The Journal of Chemical Physics,* **127(23):** 234903 (2007).

[26] Storn R., Price K., Differential Evolution – a Simple and Efficient Heuristic for Global Optimization over Continuous Spaces, *Journal of Global Optimization,* **11(4):** 341-359 (1997).

[27] Kim J.E., Kang J.W., Lim J.S., Measurement of CO_2 Solubility in Cyanide Anion Based Ionic Liquids; $[C_4mim][SCN]$, $[C_4mim][N(CN)_2]$, $[C_4mim][C(CN)_3]$, *Korean Journal of Chemical Engineering,* **32(8):** 1678-1687 (2015).

[28] Carvalho P.J., Álvarez V.H., Marrucho I.M., Aznar M., Coutinho J.A.P., High Pressure Phase Behavior of Carbon Dioxide in 1-Butyl-3-Methylimidazolium Bis(Trifluoromethylsulfonyl)Imide and 1-Butyl-3-Methylimidazolium Dicyanamide Ionic Liquids, *The Journal of Supercritical Fluids,* **50(2):** 105-111 (2009).

[29] Zubeir L.F., Romanos G.E., Weggemans W.M.A., Iliev B., Schubert T.J.S., Kroon M.C., Solubility and Diffusivity of CO_2 in the Ionic Liquid 1-Butyl-3-Methylimidazolium Tricyanomethanide Within a Large Pressure Range (0.01 Mpa to 10 Mpa), *Journal of Chemical & Engineering Data,* **60(6):** 1544-1562 (2015).

[30] Mota-Martinez M.T., Althuluth M., Kroon M.C., Peters C.J., Solubility of Carbon Dioxide in the Low-Viscosity Ionic Liquid 1-Hexyl-3-Methylimidazolium Tetracyanoborate, *Fluid Phase Equilibria,* **332:** 35-39 (2012).

[31] Aki S.N.V.K., Mellein B.R., Saurer E.M., Brennecke J.F., High-Pressure Phase Behavior of Carbon Dioxide with Imidazolium-Based Ionic Liquids, *The Journal of Physical Chemistry B,* **108(52):** 20355-20365 (2004).

[32] Cho H.-K., Kim J.E., Lim J.S., The Effect of Cyano Groups on the Solubility of Carbon Dioxide in Ionic Liquids Containing Cyano Groups in Anion, *Korean Journal of Chemical Engineering,* **34(5):** 1475-1482 (2017).

[33] Zakrzewska M.E., Nunes da Ponte M., Volumetric and Phase Behaviour of Mixtures of Tetracyanoborate-Based Ionic Liquids with High Pressure Carbon Dioxide, *The Journal of Supercritical Fluids,* **113:** 31-38 (2016).